Published in final edited form as:

J Electroanal Chem (Lausanne). 2011 June 15; 656(1-2): 106–113. doi:10.1016/j.jelechem.2010.12.031.

Simultaneous real-time measurement of EEG/EMG and L-glutamate in mice: A biosensor study of neuronal activity during sleep

Erik Naylor[a], **Daniel V. Aillon**[a], **Seth Gabbert**[a], **Hans Harmon**[a], **David A. Johnson**[a], **George S. Wilson**[b,*], and **Peter A. Petillo**[a,*]

[a]Pinnacle Technology Inc., 2721 Oregon Street, Lawrence, KS 66046, United States

[b]Department of Chemistry, Malott Hall, Room 3027, University of Kansas, Lawrence, KS 66045, United States

Abstract

We report on electroencephalograph (EEG) and electromyograph (EMG) measurements concurrently with real-time changes in L-glutamate concentration. These data reveal a link between sleep state and extracellular neurotransmitter changes in a freely-moving (tethered) mouse. This study reveals, for the first time in mice, that the extracellular L-glutamate concentration in the pre-frontal cortex (PFC) increases during periods of extended wakefulness, decreases during extended sleep episodes and spikes during periods of REM sleep. Individual sleep epochs (10 s in duration) were scored as wake, slow-wave (SW) sleep or rapid eye movement (REM) sleep, and then correlated as a function of time with measured changes in L-glutamate concentrations. The observed L-glutamate levels show a statistically significant increase of 0.86 ± 0.26 μM ($p < 0.05$) over 37 wake episodes recorded from all mice ($n = 6$). Over the course of 49 measured sleep periods longer than 15 min, L-glutamate concentrations decline by a similar amount (0.88 ± 0.37 μM, $p < 0.08$). The analysis of 163 individual REM sleep episodes greater than one min in length across all mice ($n = 6$) demonstrates a significant rise in L-glutamate levels as compared to the 1 min preceding REM sleep onset (RM-ANOVA, DF = 20, $F = 6.458$, $p < 0.001$). The observed rapid changes in L-glutamate concentration during REM sleep last only between 1 and 3 min. The approach described can also be extended to other regions of the brain which are hypothesized to play a role in sleep. This study highlights the importance of obtaining simultaneous measurements of neurotransmitter levels in conjunction with sleep markers to help elucidate the underlying physiological and ultimately the genetic components of sleep.

Keywords

Glutamate biosensor; Electroencephalography; Electromyography; Mouse sleep studies; Continuous *in vivo* monitoring

*Corresponding authors. Tel.: +1 785 864 5152; fax: +1 785 864 5396 (G.S. Wilson), tel.: +1 785 832 8866 (P.A. Petillo). gwilson@ku.edu (G.S. Wilson), alchmist@pinnaclet.com (P.A. Petillo).

1. Introduction

Electrophysiological studies aimed at elucidating the role of sleep in mammals are nearly a century old, and yet the function of sleep remains an elusive mystery [1]. Discrimination of sleep state activity relies on the accurate determination of electroencephalograph (EEG) and electromyograph (EMG) signals from a freely moving animal. EEG recordings of the brain yield a wealth of information regarding neuronal activity, but are limited in that these measurements only report gross neuronal firing patterns. Understanding the underlying physiology driving these large-scale neuronal events requires techniques that can accurately monitor neurochemical release and uptake. Such techniques can target specific structures within the brain to complement electrophysiological studies and are now recognized as an important component to investigating the role of sleep [2].

The predominant approach for the accurate determination of sleep state requires simultaneous EEG recordings from cortical regions of the brain and concurrent measurement of muscle EMG activity [3]. EEG traces reflect microvolt potential differences between two independent electrodes implanted in the skull. Potential differences ranging in size from 50 to 200 μV arise as a result of changes in membrane potentials due to neuronal firing activity. The frequency of EEG signals also reflects neuronal activity. High frequency (>12 Hz) EEG indicates active, disparate neuronal activation typically associated with waking. High amplitude (>100 μV), low frequency (<5 Hz) EEG activity, such as that observed during slow-wave (SW) sleep, represents cortical neurons firing in a highly synchronized rhythm. EEG traces with an abundance of 5–8 Hz frequencies whose amplitudes are <100 μV typically characterize rapid eye movement (REM) sleep. EMG activity, measured by placing two independent electrodes in muscle, reflects the electrical potential arising from the neuronal activation associated with muscle contraction. High amplitude EMG reflects active movement while a tonic EMG signal indicates quiescence or sleep [4].

Although measurement of brain and muscle electrical activity can indicate sleep states, it provides no indication of neurochemistry function. A better understanding of sleep physiology requires simultaneous measurements of neurotransmitter activity alongside EEG recordings. L-Glutamate, the most abundant excitatory neurotransmitter in the brain, is believed to play an important, but as yet undefined role during sleep. Previous studies in rats have shown altered L-glutamate levels between sleep/wake states [5] and increased extracellular L-glutamate concentration in the prefrontal cortex region during REM sleep [6].

Quantifying neurotransmitter concentration as a function of time concurrently with sleep is non-trivial. Traditionally, this sampling is accomplished using microdialysis [7], or post-mortem techniques such as immunohistochemistry [8] or autoradiography [9]. Each of these techniques can provide useful data, but all suffer from similar limitations including the inability to monitor neurotransmitters in real-time (e.g. a lack of temporal resolution), and perturbation of the nascent equilibrium of the space being monitored (local environment). For example, microdialysis provides sampling over hours or days, but is typically limited to a rate no faster than 1–5 min per sample [5,10]. During microdialysis, removal of the analyte

from the local environment perturbs the natural equilibrium and post-collection processing of samples is laborious. Post-mortem techniques suffer from the extreme limitation of yielding only a single usable time point per animal and the necessary step of sacrifice interferes with measurement of sleep [8b]. The use of non-invasive techniques, such as MRI concurrently with EEG recording, have also been attempted, but these techniques require that the animal remain immobilized throughout the sampling period [11].

The simultaneous measurement of EEG, EMG and L-glutamate biosensor recordings is well-suited for quantifying second-by-second changes in neurotransmitter release during sleep in a manner that does not perturb the equilibrium of the local environment [12]. Biosensors employ biological recognition elements, typically an enzyme, to produce an electroactive species that is then oxidized at the transducing element [12]. In the case of an L-glutamate biosensor, a Pt–Ir electrode polarized to 0.6 V is coated in a matrix containing the biological element L-glutamate oxidase. L-Glutamate in the extracellular space surrounding the biosensor is converted to hydrogen peroxide (H_2O_2) by L-glutamate oxidase. The enzymatically-produced H_2O_2 then diffuses through various membrane layers to the Pt–Ir surface where it is oxidized to produce a measureable amperometric current [15].

Recent studies highlight the effectiveness of combining EEG and EMG recordings coupled with simultaneous biosensor measurements in a rat model [5,6,13]. These studies report elevation in glutamatergic activity during wake [6] and significant rises in L-glutamate levels during REM sleep episodes [10]. Without exception, all of these studies have been conducted using rats as the model organism. Rats are advantageous for physiological studies due to their size, but the results of these studies are difficult to leverage into the underlying genetics. The mouse, by virtue of its use as a genetic model, is a far more powerful means to investigate sleep [14].

Herein, we report on the measurement of EEG and EMG concurrently with real-time changes in L-glutamate concentration. These data reveal a link between sleep state and extracellular neurotransmitter changes in a freely-moving (tethered) mouse. A smaller subject (mouse vs. rat) demands further miniaturization of the data acquisition system. The *in vivo* measurement of L-glutamate is particularly challenging because of its low basal levels (~10 μM) [16]. L-Glutamate biosensors used in this study address this issue by harnessing the innate efficiency, activity, and specificity of the biological recognition element (L-glutamate oxidase) to provide high sensitivity. The biosensors are necessarily selective, rejecting significant potential interferences such as L-ascorbate. This study reveals, for the first time in mice, that the extracellular L-glutamate concentration in the pre-frontal cortex increases during periods of extended wakefulness, decreases during extended sleep episodes and spikes during periods of REM sleep.

2. Experimental

2.1. Animals

Six young (12–16 wks) male wild-type C57Bl6 mice were obtained from Jackson Laboratories (Bar Harbor, ME) and housed under a 12 h light/12 h dark cycle (LD 12:12) for

at least 3 weeks prior to surgery. All mice remained on LD 12:12 throughout the experiment with food and water available *ad lib*. All animal procedures were approved by the University of Kansas Animal Care and Use Committee.

2.2. Surgery

Mice were anesthetized using ketamine (100 mg/kg)/xylazine (10 mg/kg) and surgically implanted with electrodes for EEG and EMG recording along with an indwelling cannula for later biosensor implantation (Fig. 1). One stainless steel screw with an attached wire (Part #8403, Pinnacle Technology, Inc., Lawrence, KS) was positioned in the frontal region (A/P: −1.0 mm, M/L −1.5 mm) and two screws with wires were positioned over the posterior brain (A/P: −3.0 mm, M/L ±1.5 mm). EMG activity was monitored using dual Pt–Ir electrodes, partially coated with Teflon (Part #10IR5T, MedWire Mt.Vernon, NY), inserted bilaterally into the neck/back region (nuchal) muscles. All electrode leads were connected to a pre-manufactured headmount (Part #8402, Pinnacle Technology, Inc., Lawrence, KS) and sealed with dental acrylic resin. A cannula for biosensor insertion (ID ~400 μm) (Part #MD-2255, BASi, West Lafayette, IN) was implanted in the pre-frontal cortex (A/P: +1.94 mm, M/L −1.50 mm, D/V −0.5 mm). Accuracy of the sensor placement was confirmed through visual examination of brain tissue during post-mortem analysis.

2.3. Biosensor construction

Glutamate biosensors obtained from Pinnacle Technology, Inc. (Part #7004-Glutamate, Lawrence, KS) were constructed according to previously published methods [16]. Briefly, the working electrode is formed by a Teflon-coated Pt–Ir wire (90% Pt, 10% Ir, Medwire, Mount Vernon, NY). A silver wire (Medwire, Mount Vernon, NY) is wrapped concentrically around the Pt–Ir wire and charged by oxidation in a $FeCl_3$ (0.3 M in 0.1 M aqueous HCl) solution forming the AgCl reference electrode. At the distal end of the working electrode, a 1 mm section is exposed to form the sensing cavity.

To protect the electrode surface from endogenous electroactive species (i.e. ascorbic acid), a selective membrane is cast over the surface of the working electrode. Ascorbic acid, a very predominant interferent encountered in mammalian brains [16,17] can reach concentrations as high as 300 μM. Electroactive interferents are excluded by the presence of a semi-permeable membrane that allows the diffusion of H_2O_2 while retarding larger and negatively charged compounds. Assessment of likely interferences has been previously published [16a]. Additionally, L-ascorbate oxidase (EC 1.10.3.3) is co-immobilized with L-glutamate oxidase (EC 1.4.3.11) in the sensing cavity to actively remove L-ascorbate from the local environment (Fig. 2). A head-piece and connector coupled with a guide cannula is used for support in *in vivo* implantation. All biosensors are calibrated *in vitro* prior to implantation and after explantation.

2.4. Biosensor measurements

In vivo use of biosensors for detection of L-glutamate has been previously described [5,16a]. In this study, the L-glutamate biosensor was inserted into the guide cannula to extend 1 mm into the brain tissue below the cannula tip. Experiments were initiated at the onset of the “lights-off” period which coincided with the insertion of the biosensor. Amperometric

biosensor readings were collected once a second over the entire course of the experiment (total of 24 h of data collection), the first 12 h of which constituted the run-in period for *in vivo* stabilization of the biosensor. The biosensor measures L-glutamate in the extracellular fluid (ECF) of the brain. All biosensors were explanted through the guide cannula following the end of the experiment and immediately (<10 min) post-calibrated in a 37 °C bath containing 100 mM PBS (pH 7.4) buffer solution. Titration of the biosensor response was accomplished by stepwise addition of L-glutamate (10 μM) at regular intervals as for the pre-calibration (Fig. 3). Amperometric changes in individual biosensor readings were used to calculate concentration changes *in vivo*.

It should be noted that it is difficult, if not impossible, to perform an *in vivo* calibration of a biosensor when implanted in the brain of a conscious, freely moving (tethered) animal. Instead, the biosensor must be calibrated *in vitro* (Fig. 3), yet the calibration must still reflect its *in vivo* sensitivity which is typically up to 60% less than its pre-implantation sensitivity [16a]. This loss of sensitivity is due to bio-fouling and tissue stabilization that occur during the run-in period when the biosensor is equilibrating with its environment. Following this period, the *in vivo* sensitivity and selectivity of the biosensor is stable for at least 24 h. In order to determine the *in vivo* sensitivity over this time period, the biosensor is explanted at the conclusion of the experiment and immediately calibrated *in vitro*. When performed quickly (moving the biosensor from 'brain-to-beaker') this 'post-calibration' provides an excellent estimation of the biosensor *in vivo* sensitivity [18]. It has also been previously demonstrated that a "sentinel" electrode, one containing no enzyme, shows no response during stimulated glutamate release in the hippocampus [16a].

By calibrating each biosensor after explantation, the recorded *in vivo* current can be transformed into meaningful changes in L-glutamate concentration even though implantation can result in a 50% loss of sensitivity. Thus, multiple biosensors implanted in multiple animals are now directly comparable. The effectiveness of the L-ascorbate oxidase and interference membranes is also assessed during post-calibration via a single 250 μM injection of L-ascorbic acid [16a]. There may be some degradation of selectivity with respect to L-ascorbate, which translates into a slowly rising baseline. This does not materially affect calibration.

2.5. EEG/EMG data collection

A pre-amplifier unit (Part #8406-SL, Pinnacle Technology, Inc., Lawrence, KS), rigidly attached to the mouse headmount, provided first stage amplification (100×) and initial high-pass filtering (first-order 0.5 Hz for EEG and 10 Hz for EMG). The signals were then routed to an 8401 conditioning/acquisition system (Pinnacle Technology, Inc., Lawrence, KS) via a tether and low-torque commutator (Part #8408, Pinnacle Technology, Inc., Lawrence, KS). The 8401 amplifier/conditioning unit provided an additional 50× signal amplification, additional high-pass filtering, and an 8th order elliptic low pass filter (50 Hz EEG and 200 Hz EMG). The signals were then sampled at 500 Hz, digitized using a 14 bit A/D converter and routed to a PC based acquisition and analysis software package via USB.

By nature, mice are nocturnal and their circadian rhythm is such that the majority of wake activity is seen during periods of "lights-off". Sleep and specifically REM sleep are typically

observed during “lights-on” periods. EEG, EMG and biosensor signals were continuously collected for a 24 h period following biosensor insertion at the start of the “lights-off” period. The first 12 h of the experiment (“lights-off”) were dedicated to sensor run-in and establishment of a stable biosensor signal. During the next 12 h (“lights-on”), corresponding to the period with the highest amount of SW and REM sleep, EEG, EMG and L-glutamate biosensor data were collected for analysis.

2.6. Sleep/wake analysis

Continuous sections of recorded EEG and EMG data were broken into discrete periods (epochs) lasting 10 s. Each 10 s epoch was classified as wake, SW or REM sleep based on which type of waveform occupied >50% of that time (Fig. 4a). This particular choice of sampling window is an optimal tradeoff between having sufficient data to make an accurate state determination and providing a dataset that can be sufficiently manipulated by a human scorer. First-pass scoring was accomplished using a cluster scoring method based on visual clustering similar to that described by Benington et al. [19]. Cluster scoring helps define the transition epochs which are then scored as wake, SW sleep or REM sleep by human visual pattern recognition. Post-scoring data processing utilized the PAL-8200 analysis package (Pinnacle Technology, Inc. Lawrence, KS). Final sleep state determination of any epoch which was not clearly delineated by the cluster method was scored through visual examination.

Fig. 4a shows the EEG/EMG data from the three states, wake, SW and REM. An examination of the EMG signal clearly distinguishes the two sleep states from the wake state, where the movement of the mouse causes large changes in the observed EMG amplitudes and frequencies. The residual signal in the two sleep states is largely due to the measurement of heart beat. The EEG-1 and EEG-2 amplitudes measured in the same mouse are different, largely due to the dissimilar spatial orientation between the two electrodes and the EEG common electrode (Fig. 1b). Qualitatively, SW sleep is of a lower frequency than either the wake or, more importantly, REM sleep (Fig. 4b). An expanded 10 s (one epoch) view of SW and REM sleep EEG-2 waveforms shows that the majority of frequencies that comprise SW sleep fall into the 1–4 Hz frequency range. The SW sleep epoch also shows a significantly larger EEG-2 amplitude than either wake or REM sleep. By contrast, REM sleep exhibits a predominance of 5–8 Hz activity and an amplitude that is visually lower than SW sleep.

2.7. Determination of sleep and wake episodes for the purpose of L-glutamate analysis

Wake episodes were globally classified as periods of at least 15 min in length where no more than five continuous minutes of SW sleep was present. A wake episode was considered terminated when five or more continuous minutes of sleep (SW or REM) were observed. Sleep episodes were globally classified as at least 15 min of continuous sleep with both SW and REM sleep epochs contributing as part of the same sleep episode. A sleep episode was considered terminated when five or more continuous minutes of wake activity were observed. REM sleep periods longer than 1 min were disregarded at the end of sleep episode. Based on these criteria, the average episode lengths were 32.3 min (wake) and 60.1

min (sleep), consistent with the “lights-on” period demonstrating enhanced periods of SW and REM sleep.

Biosensor measurements were determined by averaging L-glutamate biosensor readings during the first 5 min (baseline value) and the last 5 min (terminal value) of each episode. The change during a scored episode was recorded as the difference between the baseline and terminal values. Due to the shortened nature of REM episodes, a slightly different method was employed. Characterizing REM sleep periods within a sleep episode presents a special problem because REM periods have durations of less than 3 min. For REM sleep periods lasting longer than 1 min, a baseline was established by averaging L-glutamate concentrations for the minute immediately prior to the onset of the REM sleep episode. The baseline was then subtracted from the L-glutamate concentration during each epoch of the REM sleep episode.

3. Results and discussion

This study presents the first concurrent measurements of EEG and EMG activity along with simultaneous real-time biosensor recordings in the pre-frontal cortex (PFC) of a mouse. This technique provides an unprecedented window into the neurochemistry associated with the sleeping brain. The key finding of this study is the consistent fluctuation of L-glutamate levels (Fig. 5) in the PFC of a mouse during sleep/wake cycles. Gross correlations between all six animals are readily apparent. When scored episodes are aggregated, rising L-glutamate levels are noted during extended (>15 min) waking periods. By contrast, long periods of sleep (>15 min of combined SW and REM sleep) demonstrate an overall decline in brain ECF L-glutamate concentration (Fig. 6). The observed L-glutamate levels show a statistically significant increase of 0.86 ± 0.26 μM ($p < 0.05$) over 37 wake episodes recorded from all mice ($n = 6$). Over the course of 49 measured sleep periods longer than 15 min, L-glutamate concentrations decline by a similar amount (0.88 ± 0.37 μM, $p < 0.08$). Interestingly, sleep and waking episodes <15 min lack a consistently recognizable pattern. Despite the recognized importance of L-glutamate as the major excitatory neurotransmitter in the brain, changes in L-glutamate concentrations do not occur without concomitant changes in brain metabolism directly related to energy use [25]. The simultaneous measurement of multiple brain analytes in conjunction with electrophysiological activity hold the promise to further unravel these complex and highly intertwined relationships.

Unlike SW sleep, REM sleep demonstrates very different brain wave patterns and is generally believed to reflect a period of increased cortical activity distinct from that observed during SW sleep. Not surprisingly, a different temporal L-glutamate pattern is clearly seen during REM sleep. As shown in Fig. 7, the analysis of 163 individual REM sleep episodes greater than one min in length across all mice ($n = 6$) demonstrates a significant rise in L-glutamate levels as compared to the 1 min preceding REM sleep onset (RM-ANOVA, DF = 20, $F = 6.458$, $p < 0.001$). The observed rapid changes in L-glutamate concentration during REM sleep last only between 1 and 3 min. Visualization of this REM sleep related L-glutamate concentration change has only recently been possible through the use of biosensors employing a rapid (1 Hz) sampling rate. One study [10] employing 1 min microdialysis sampling from the orbitofrontal cortex of rats reported REM sleep related L-

glutamate increases. However, microdialysis studies employing lower sampling frequencies (on the order of minutes) likely missed this phenomenon. Unlike the Lopez-Rodriguez report [10], the use of biosensors with the characteristics described in the present report allow for the direct visualization of discrete events during REM sleep episodes with a 1 s temporal resolution [16a] that is currently unattainable by routine microdialysis.

Very similar temporal changes in L-glutamate levels during REM sleep have been reported in biosensor studies in rats [5,6]. Our findings in mice support the hypothesis that these changes in L-glutamate levels are not an isolated phenomenon of a particular rodent model but may reflect a fundamental mechanism underlying REM sleep. Following release, L-glutamate is rapidly cleared from the synaptic cleft [20]. Increasing L-glutamate concentration as measured by the biosensor indicates an increase in L-glutamate release, lowered L-glutamate uptake or a combination of these two factors. Other researchers have noted rapid rises in L-glutamate concentration during REM sleep [6,10] and active waking episodes [5]. L-Glutamate uptake has been shown to be inhibited by the infusion of L-glutamate via a microdialysis probe [21] and Kullmann et al. [22] have demonstrated that released extracellular L-glutamate can spill-over and occupy neighboring synapses, thus eliciting further L-glutamate release. Taken together, these findings suggest that extracellular L-glutamate concentrations are continually rising during REM sleep while L-glutamate uptake is limited or hindered. The neurotoxic nature of exogenous extracellular L-glutamate is well established as a mechanism of cell death [23] and it may be that REM sleep periods in rodents are limited to short durations to prevent excessive extracellular L-glutamate build-up as a neuroprotective measure.

4. Conclusions

L-Glutamate is the most abundant excitatory neurotransmitter in the mammalian CNS, occupying 90% of all cortical synapses [24]. It should not be surprising that glutamatergic transmission represents most of the energy expenditure in the brain [25]. Astrocytes respond to L-glutamate release by a cascade of events designed to rapidly increase the available pool of energy substrates. Exogenous application of L-glutamate to astrocytes has been demonstrated to induce a rapid and reversible increase in glucose transport [26] caused by Na^+ influx occurring concurrently with astrocytic L-glutamate uptake [27]. The Na^+ rise induces activation of Na+/K+ ATPase resulting in the glycolytic processing of glucose to lactate [28]. Thus, it may be possible to relate extracellular L-glutamate levels as a byproduct of glutamatergic synaptic activity. This may further be postulated to act as a proxy for determination of local neuronal and astrocytic metabolism [29].

The fluctuations in L-glutamate levels in the PFC during sleep and wake episodes are strikingly parallel to those previously reported in the PFC of rats [6]. These results in both mice and rats suggest that L-glutamate may be fulfilling similar roles during sleep and waking across species. Such a relationship hints at the presence of a modulatory role between L-glutamate levels and sleep, the nature of which remains to be fully described. The approach described herein can also be extended to other regions of the brain which are hypothesized to play a role in sleep. This study highlights the importance of obtaining

simultaneous measurements of neurotransmitter levels in conjunction with sleep markers to help elucidate the underlying physiological and ultimately the genetic components of sleep.

Acknowledgments

We would like to thank Bailey Knott and Toni Brou and for their assistance in creating Figs. 1 and 2 respectively, Brian Barrett for assistance with Fig. 3, and Donna A. Johnson and Chris Jubic for useful discussions. This research was supported by Grant #5R44MH076318-03 from the National Institute of Mental Health. The content is solely the responsibility of the authors and does not necessarily represent the official views of the National Institute of Mental Health or the National Institutes of Health.

Biographies

Erik Naylor received his B.S. degree in Biology from Virginia Tech in Blacksburg, VA, and his doctorate in Neuroscience at Northwestern University in Evanston, IL where he investigated genetic components common to sleep and circadian rhythms. His postdoctoral work at Northwestern Memorial Hospital focused on Circadian Rhythm Sleep Disorders. Erik is currently the Director of Biomedical Research at Pinnacle Technology, Inc. in Lawrence Kansas. His research interests include investigation of the neurochemical processes of sleep, circadian rhythm physiology and preclinical biomedical instrumentation design.

Daniel V. Aillon completed his undergraduate degree in biochemistry at the University of Kansas in 2001. He joined Pinnacle Technology Inc. in 2002 where he worked closely with Dr. George Wilson at The University of Kansas to transfer Dr. Wilson's biosensor technology from the laboratory to Pinnacle. In 2004, the commercialized biosensor was introduced to the market. In 2008 Daniel was made Director of Biosensor Technology at Pinnacle.

Seth Gabbert received his bachelor's degree in Computer Engineering in 2001 from the University of Kansas. He joined Pinnacle Technology full time after graduation. He specializes in electronics and firmware design.

Hans Harmon acquired his B.S in Computer Engineering at KU in 2001, M.S. in Computer Engineering at KU in 2004, specializing in robotics. He has since worked at Pinnacle Technology as a senior software engineer.

David A. Johnson received his Ph.D. in 1989 in Electrical Engineering from Arizona State University. From 1990 to 1995 he was an Associate Professor of Engineering Physics at Kettering University in Michigan. In 1995, he left academia (with tenure) and went to work for industry, first as a Senior Process Engineer for Microchip Technology (Tempe, AZ) and then, since 1996, as Chief Technical Officer for Pinnacle. He specializes in biomedical devices, wireless systems and industrial control systems.

George S. Wilson received his A.B. degree in Chemistry at Princeton University and his Ph.D. at the University of Illinois. Following a 2-year postdoctoral stay in biochemistry, he joined the Chemistry Department at the University of Arizona. In 1987 he was appointed Higuchi Distinguished Professor of Chemistry and Pharmaceutical Chemistry at the University of Kansas. From 2004–2010, he served as Associate Vice Provost for Research and Graduate Studies, when he retired from the University. He served as the Chairman of the Electrochemistry Commission and President of the Physical and Biophysical Chemistry Division of IUPAC. He is a Fellow of the AAAS, Fellow of the International Society of Electrochemistry, and a winner of the C. N. Reilley Award in Electroanalytical Chemistry. His research interests are in the area of real-time in vivo monitoring using biosensors, analytical applications of biological recognition, and the redox chemistry of biologically important molecules.

Peter A. Petillo received his B.S. degree in chemistry from the University of New Hampshire in 1985 and his Ph.D. in organic chemistry from the University of Wisconsin at Madison in 1991. After postdoctorals at the University of Wisconsin and the Whitehead Institute for Biomedical Research, he moved to the University of Illinois, Champaign-Urbana, where his research group developed new paramagnetic contrast agents for MRI imaging and robust synthetic methods for the assembly of bio-active agents including peptides and carbohydrates. He was a founder and the Chief Science officer of Deciphera Pharmaceuticals before joining Pinnacle Technology, Inc. in 2010 as the Chief Science Officer. His research interests are in energy utilization in biological systems, biopolymer folding, biological recognition, and the synthetic and biosynthetic construction of biologically important molecules.

References

1. Dement, WC. History of sleep physiology and medicine. In: Kryger, MH.; Roth, T.; Dement, WC., editors. Principles and Practices of Sleep Medicine. fourth. W.B. Saunders Company; Philadelphia: 2005. p. 1-12.

2. Zepelin, H.; Siegel, JM.; Tobler, I. Mammalian sleep. In: Kryger, MH.; Roth, T.; Dement, WC., editors. Principles and Practices of Sleep Medicine. fourth. W.B. Saunders Company; Philadelphia: 2005. p. 91-100.
3. Steriade, M. Brain electrical activity and sensory processing during waking and sleep states. In: Kryger, MH.; Roth, T.; Dement, WC., editors. Principles and Practices of Sleep Medicine. fourth. W.B. Saunders Company; Philadelphia: 2005. p. 91-100.
4. Carskadon, MA.; Dement, WC. Normal human sleep: an overview. In: Kryger, MH.; Roth, T.; Dement, WC., editors. Principles and Practices of Sleep Medicine. W.B. Saunders; Philadelphia: 1994. p. 889-913.
5. John J, Ramanathan L, Siegel JM. Am J Physiol Regul Integr Comp Physiol. 2008; 295(6):R2041–R2049. [PubMed: 18815208]
6. Dash MB, Douglas CL, Vyazovskiy VV, Cirelli C, Tononi G. J Neurosci. 2009; 29(3):620–629. [PubMed: 19158289]
7. (a) Alam MN, Szymusiak R, Gong H, King J, McGinty D. J Physiol. 1999; 521(Pt 3):679–690. [PubMed: 10601498] (b) Basheer R, Porkka-Heiskanen T, Stenberg D, McCarley RW. Brain Res Mol Brain Res. 1999; 73(1–2):1–10. [PubMed: 10581392] (c) Nitz D, Siegel JM. Neuroscience. 1997; 78(3):795–801. [PubMed: 9153658] (d) Porkka-Heiskanen T, Strecker RE, Thakkar M, Bjorkum AA, Greene RW, McCarley RW. Science. 1997; 276(5316):1265–1268. [PubMed: 9157887]
8. (a) Hagan JJ, Leslie RA, Patel S, Evans ML, Wattam TA, Holmes S, Benham CD, Taylor SG, Routledge C, Hemmati P, Munton RP, Ashmeade TE, Shah AS, Hatcher JP, Hatcher PD, Jones DN, Smith MI, Piper DC, Hunter AJ, Porter RA. N Upton, Proc Natl Acad Sci USA. 1999; 96(19): 10911–10916.(b) Ko EM, Estabrooke IV, McCarthy M, Scammell TE. Brain Res. 2003; 992(2): 220–226. [PubMed: 14625060]
9. (a) Franken P, Gip P, Hagiwara H, Ruby NF, Heller HC. Am J Physiol Regul Integr Comp Physiol. 2003; 285(2):R413–R419. [PubMed: 12730076] (b) Gip P, Hagiwara G, Ruby NF, Heller HC. Am J Physiol Regul Integr Comp Physiol. 2002; 283(1):R54–R59. [PubMed: 12069930] (c) Ramm P, Frost BJ. Sleep. 1983; 6(3):196–216. [PubMed: 6622878]
10. Lopez-Rodriguez F, Medina-Ceja L, Wilson CL, Jhung D, Morales-Villagran A. Arch Med Res. 2007; 38(1):52–55. [PubMed: 17174723]
11. Khubchandani M, Mallick HN, Jagannathan NR, Mohan Kumar V. Magn Reson Med. 2003; 49(5): 962–967. [PubMed: 12704780]
12. Wilson GS, Johnson MA. Chem Rev. 2008; 108(7):2462–2481. [PubMed: 18558752]
13. (a) Netchiporouk L, Shram N, Salvert D, Cespuglio R. Eur J Neurosci. 2001; 13(7):1429–1434. [PubMed: 11298804] (b) Shram N, Netchiporouk L, Cespuglio R. Eur J Neurosci. 2002; 16(3): 461–466. [PubMed: 12193189]
14. (a) Friedman JK. Physiol Behav. 1974; 12:169–175. [PubMed: 4361192] (b) Shaw PJ, Franken P. J Neurobiol. 2003; 54(1):179–202. [PubMed: 12486704] (c) Valatx JL, Bugat R. Brain Res. 1974; 69(2):315–330. [PubMed: 4362814]
15. Wilson GS, Gifford R. Biosens Bioelectron. 2005; 20(12):2388–2403. [PubMed: 15854814]
16. (a) Hu Y, Mitchell KM, Albahadily FN, Michaelis EK, Wilson GS. Brain Res. 1994; 659(1–2): 117–125. [PubMed: 7820652] (b) Wilson GS, Bindra DS, Hill BS, Thévenot DR, Sternberg R, Reach G, Zhang Y. Implantable Glucose Sensor 51,65,407. 1992
17. Rebec GV, Witowski SR, Sandstrom MI, Rostand RD, Kennedy RT. Neurosci Lett. 2005; 378(3): 166–170. [PubMed: 15781152]
18. Thomé-Duret V, Aussedat B, Reach G, Gangnerau MN, Lemonnier F, Klein JC, Zhang Y, Hu Y, Wilson GS. Metabolism. 1998; 47(7):799–803. [PubMed: 9667224]
19. Benington JH, Kodali SK, Heller HC. Sleep. 1994; 17(1):28–36. [PubMed: 8191200]
20. (a) Diamond JS, Jahr CE. J Neurosci. 1997; 17(12):4672–4687. [PubMed: 9169528] (b) Timmerman W, Westerink BH. Synapse. 1997; 27(3):242–261. [PubMed: 9329159]
21. Alexander GM, Grothusen JR, Gordon SW, Schwartzman RJ. Brain Res. 1997; 766(1–2):1–10. [PubMed: 9359581]
22. Kullmann DM, Min MY, Asztely F, Rusakov DA. Philos Trans Roy Soc Lond B Biol Sci. 1999; 354(1381):395–402. [PubMed: 10212489]

23. (a) Dirnagl U, Iadecola C, Moskowitz MA. Trends Neurosci. 1999; 22(9):391–397. [PubMed: 10441299] (b) Mergenthaler P, Dirnagl U, Meisel A. Metab Brain Dis. 2004; 19(3–4):151–167. [PubMed: 15554412]
24. Buzsaki G, Kaila K, Raichle M. Neuron. 2007; 56(5):771–783. [PubMed: 18054855]
25. (a) Sibson NR, Dhankhar A, Mason GF, Rothman DL, Behar DL, Shulman RG. Proc Natl Acad Sci USA. 1998; 95(1):316–321. [PubMed: 9419373] (b) Magistretti PJ. J Exp Biol. 2006; 209(Pt 12):2304–2311. [PubMed: 16731806]
26. Loaiza A, Porras OH, Barros LF. J Neurosci. 2003; 23(19):7337–7342. [PubMed: 12917367]
27. Pellerin L, Magistretti PJ. J Neurochem. 1997; 69(5):2132–2137. [PubMed: 9349559]
28. Pellerin L, Magistretti PJ. Dev Neurosci. 1996; 18(5–6):336–342. [PubMed: 8940604]
29. (a) Hawkins RA. Am J Clin Nutr. 2009; 90(Suppl):867S–874S. [PubMed: 19571220] (b) Magistretti PJ. Am J Clin Nutr. 2009; 90(Suppl):875S–880S. [PubMed: 19571222]

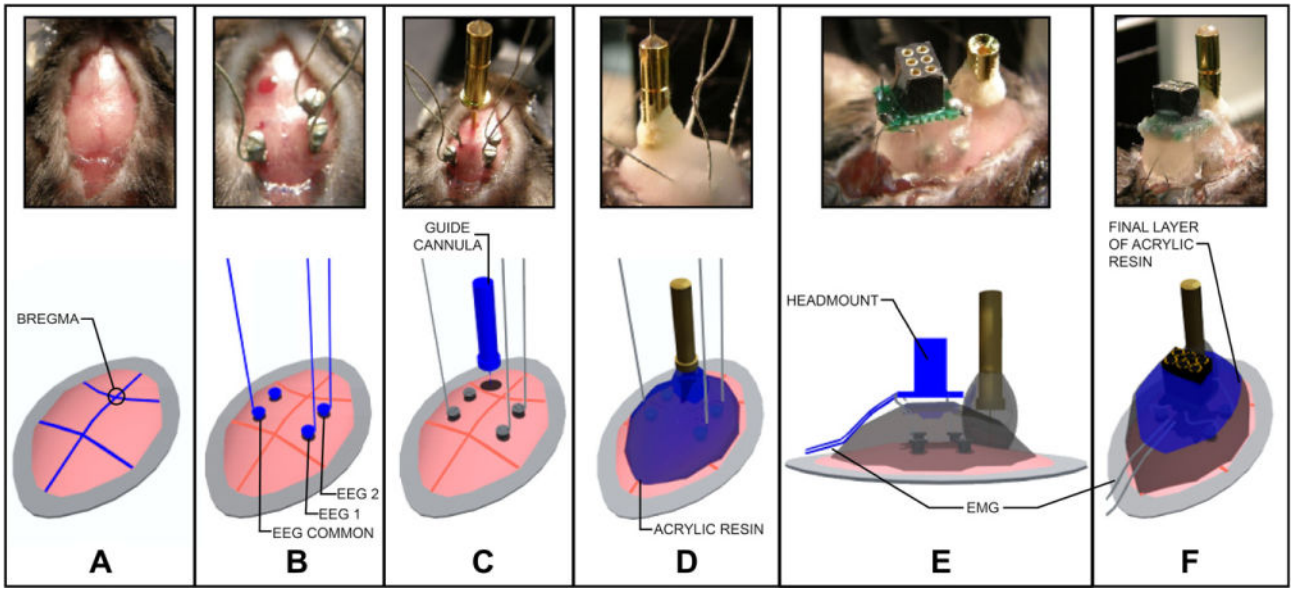

Fig. 1.

Diagrammatic representation of the EEG–EMG-biosensor surgery protocol carried out in this study. For this series, the active component in the diagram is illustrated in blue. Fig. 1a – depiction of the mouse skull after the skin was been retracted and connective tissue was removed revealing bregma, the traditional point of origin for stereotaxic coordinates. Fig. 1b – depiction of the three screws used as EEG recording electrodes. Screws for EEG-1 and EEG-2 were placed at A/P: −3.0 mm, M/L +1.5 mm and A/P: −1.0 mm, M/L +1.5 mm, respectively, while the EEG COMMON screw was located at A/P: −3.0 mm, M/L −1.5 mm. Fig. 1c – stereotaxic (measured) placement of a guide cannula at A/P: +1.94 mm, M/L −1.50 mm, D/V −0.5 mm. Fig. 1d – all items were secured in place with dental acrylic resin (blue). Fig. 1e – the connector wires for the three EEG electrodes were separately routed up through the dental acrylic resin and then soldered to the pre-fabricated headmount while Pt–Ir EMG electrodes (pre-connected to the headmount) are inserted in the nuchal (neck) muscle tissue. Fig. 1f – additional dental acrylic resin was added to the headmount and guide cannula to secure the entire assembly to the skull. (For interpretation of the references to colour in this figure legend, the reader is referred to the web version of this article.)

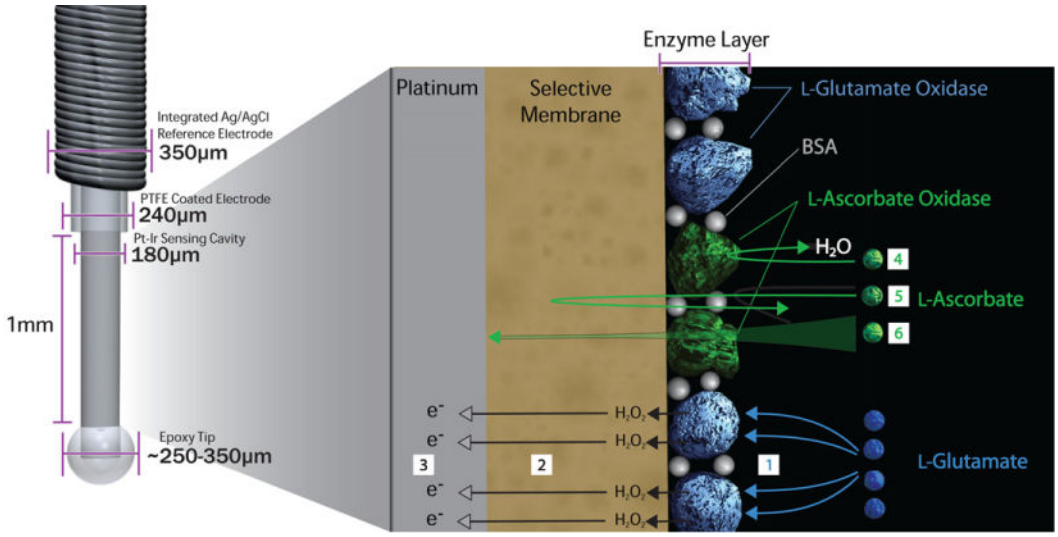

Fig. 2.

A working schematic of the L-glutamate biosensor, including biosensor dimensions. L-glutamate, in the presence of water and oxygen, is converted (Box 1) into H_2O_2, NH_3 and oxoglutaric acid by L-glutamate oxidase (EC 1.4.3.11). The enzymatically-produced H_2O_2 diffuses through the selective membrane (Box 2) to the Pt–Ir surface where it is oxidized at a potential of 0.6 V vs. Ag/AgCl (Box 3). L-Ascorbate and other electroactive interferents are excluded from the Pt–Ir surface by two mechanisms: (1) L-ascorbate oxidase (EC 1.10.3.3), in the presence of oxygen, actively removes L-ascorbate (Box 4) by conversion to dehydroascorbate and water (neither of which are electroactive at 0.6 V vs. Ag/AgCl), and (2) remaining L-ascorbate (Box 5) and other endogenous electroactive interferents are further excluded by an inner-selective membrane. While it is not possible to eliminate 100% of the electroactive interferents (Box 6), the inner-membrane and active removal of L-ascorbate effectively limit the amount of interferent that reaches the electrode surface such that any changes in the local concentration are insignificant and do not contribute to the observed current.

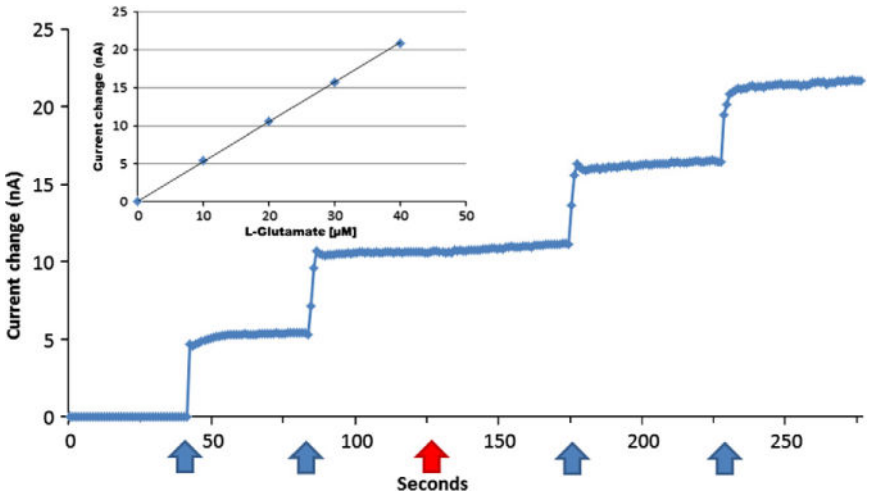

Fig. 3.

A representative *in vitro* L-glutamate biosensor pre-calibration titration graph. The biosensor was placed in a jacketed beaker previously charged with 20 ml of 100 mM PBS at ambient temperature. Stepwise titration of 10 μM L-glutamate (indicated by blue arrows) was added to the rapidly stirred PBS solution. Typically, the effectiveness of the L-ascorbate oxidase and interference membranes was assessed via a single 250 μM injection of L-ascorbic acid (red arrow). The changes in current as a function of L-glutamate concentration followed a linear pattern over a range up to 40 μM (inset graphic). The rejection ratio of L-ascorbic acid of this representative biosensor prior to implantation is over 150:1 (manufacturer specification) and is improved over the 50:1 reported elsewhere.[6] (For interpretation of the references to colour in this figure legend, the reader is referred to the web version of this article.)

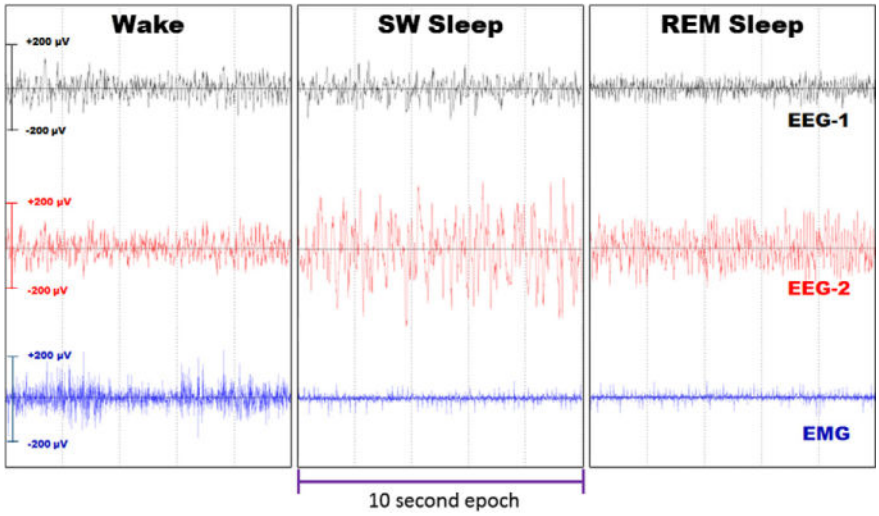

Fig. 4a.

Representative waveforms for each of the three stages of mouse sleep. Wake epochs are characterized by high amplitude EMG activity coupled with high frequency (>12 Hz) low amplitude EEG activity. SW sleep epochs are characterized by high amplitude (>100 µV), low frequency (<5 Hz) EEG activity, paired with a low amplitude EMG trace. REM sleep epochs are characterized by an abundance of 5–8 Hz frequencies (theta) in the EEG traces, whose amplitudes are <100 µV, and are coupled with a tonic EMG signal. Scoring of discrete epochs has historically been accomplished by visual recognition of these frequency and amplitude changes by a trained human scorer. Individual epochs are joined together to constitute episodes of wake, SW sleep and REM sleep. While wake and SW sleep episodes can be >15 min in length, REM sleep episodes are typically less than 3 min in duration.

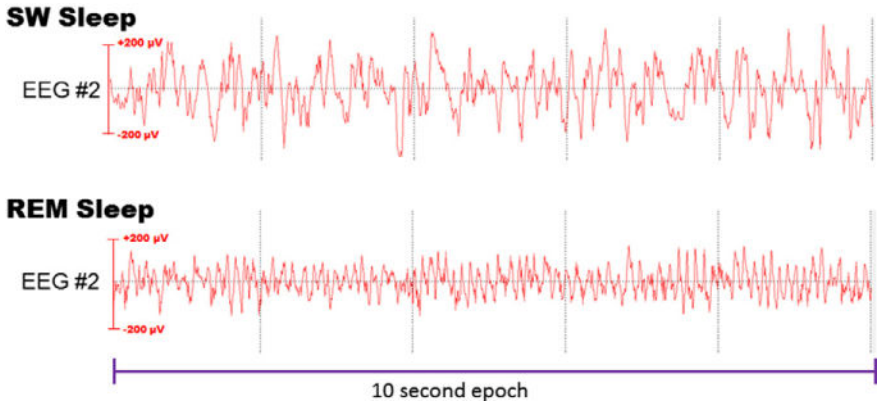

Fig. 4b.

Expanded view of a 10 s. SW and REM sleep EEG epoch. SW sleep epochs are visually determined to contain a majority of 1–4 Hz waveform activity and a significantly larger amplitude component than either wake or REM sleep epochs. By contrast, REM sleep epochs are visually inspected for a predominance of 5–8 Hz activity and an amplitude that visually corresponds to that of wake epochs.

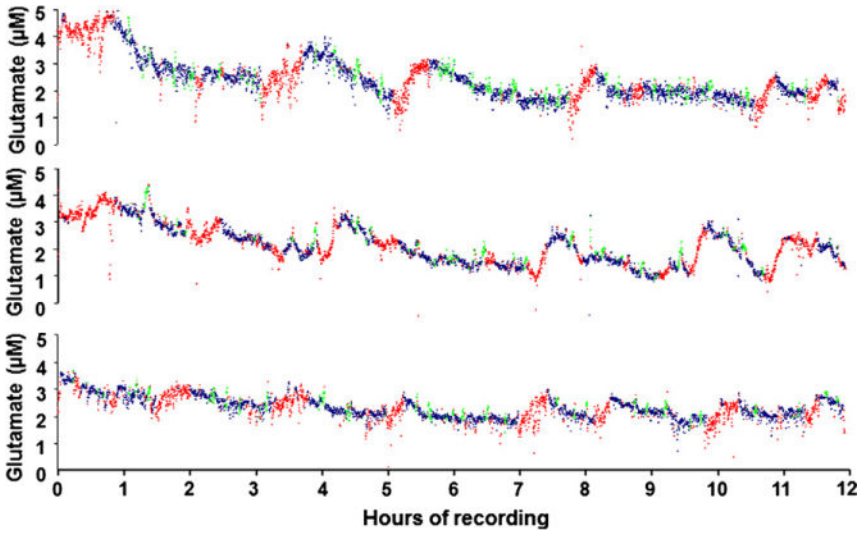

Fig. 5.

Changes in L-glutamate concentration measured concurrently with sleep state. Graphs represent three of the six mice used in this study and reflect the composite EEG/EMG/L-glutamate concentrations measured over a 12 h time period during lights-on. Individual points represent 10 s epochs with colour coding to indicate the scored sleep/wake state (Red = wake, Blue = SW sleep, Green = REM sleep). The relative changes in L-glutamate concentration on the *y*-axis are based on individual post-calibration values represented and do not denote absolute L-glutamate concentrations. Note that the green periods indicative of REM sleep events are shorter in duration than the wake or SW sleep episodes. (For interpretation of the references to colour in this figure legend, the reader is referred to the web version of this article.)

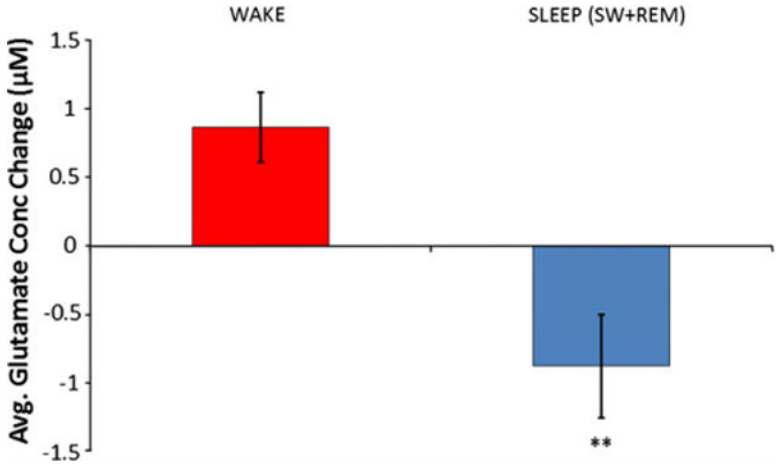

Fig. 6.

Average change in L-glutamate concentration for all wake and sleep episodes greater than 15 min in duration. Wake episodes were globally classified as periods of at least 15 min in length where no more than five continuous minutes of SW sleep was present. A wake episode was considered terminated when five or more continuous minutes of sleep (SW or REM sleep) was observed. Sleep episodes were globally classified as at least 15 min of continuous sleep with both SW and REM sleep epochs contributing as part of the same sleep episode. A sleep episode was considered terminated when five or more continuous minutes of wake activity was observed. Bars represent SEM ** = $p < 0.005$.

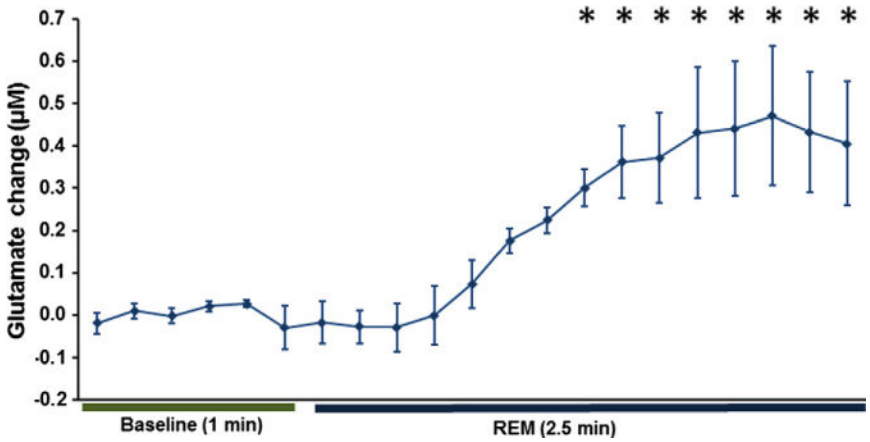

Fig. 7.

Increase in mean L-glutamate level during REM sleep episodes (163 total, $n = 6$ mice). For REM sleep periods lasting longer than 1 min, a baseline was established by averaging L-glutamate concentrations for the minute immediately prior to the onset of the REM sleep episode. The baseline was then subtracted from the L-glutamate concentration during each epoch of the REM sleep episode. Bars represent SEM, * = $p < 0.05$, Fisher's posthoc analysis RM-ANOVA, DF = 20, $F = 6.458$.